volume through which it propagates. To avoid significant pump depletion, the total energy in the laser beams must be much greater than that in the plasma wave.

The problem of producing plasmas (particularly with a cross magnetic field) with densities between $10^{16} < n_e < 10^{20}$ cm^{-3} and with the required length and homogeneity will also require considerable attention. At high intensities that are necessary in this scheme, the requirement that plasma frequency be exactly equal to the difference frequency may be relaxed, but this issue needs careful investigation.

Prospects for ultrahigh energies

High-phase velocity space charge waves in a plasma have the potential for producing the high accelerating gradients that are necessary for a new generation of particle accelerators. Whether this scheme can be used to accelerate particles to ultrahigh energies depends on how well the phase stabilization (Surfatron) scheme can be made to work in practice. Particular problems are pump depletion, filamentation of the laser and injected particle beams, and the effect of self-generated magnetic fields on the accelerating particles.

On the positive side, the Surfatron scheme would produce a compact accelerator with a high quality beam. The energy spread, $\Delta\gamma/\gamma$ would be small because approximately half of the injected particles quickly form accelerating 'buckets' that are narrow in phase space near the equilibrium point. In the wave frame this is where $\gamma_{ph}B$ is equal to the local longitudinal electric field. Thus all the particles gain energy at nearly the same rate, the one given by equation (4). The bunch length of the final beam as well as $\Delta\gamma/\gamma$ is thus expected to be extremely small, as shown in Fig. 5.

The number of accelerated particles N can be estimated from the consideration of the energy balance[6]:

$$N = 2\times10^{10}\frac{\text{laser energy (kJ)}}{\text{particle energy (GeV)}}\varepsilon\alpha\lambda_\mu\sqrt{n_{16}} \qquad (6)$$

where factor α is the ratio of particle energy to wave energy.

The zero-order motion of the particles in the Surfatron scheme is approximately a straight line, and thus synchrotron radiation loss turns out not be to be a problem. The radiation loss due to high-order bounce motion[5] and due to oscillation in the laser field, as well as other loss mechanisms such as Coulomb scattering and bremsstrahlung radiation, are also not thought to be serious problems.

Finally, the acceleration scheme is still at an embryonic stage for a reliable estimate to be made of its potential total efficiency from wall power (ac) to beam power. The severest limitation, one that is common to all laser acceleration schemes, is the a.c.-to-laser beam efficiency. If we optimistically assume this to be 10% then using our simulations as a guide we may be able to achieve a total efficiency between 10^{-3} and 10^{-4}.

We thank Professor F. F. Chen and Dr C. E. Clayton for valuable comments and discussions. This work was supported at UCLA by DOE contract DE-AM03-76SF00034, NSF grant ECS 83-10972 and LLNL University Research Program and at LANL by the DOE.

Received 11 May; accepted 6 August 1984.

1. Tajima T. & Dawson, J. M. *Phys. Rev. Lett.* **43**, 267–270 (1979).
2. Rosenbluth, M. N. & Liu, C. S. *Phys. Rev. Lett.* **29**, 701–705 (1972).
3. Joshi, C., Tajima, T., & Dawson, J. M., Baldis, H. A. & Ebrahim, N. A. *Phys. Rev. Lett.* **47**, 1285–1288 (1981).
4. Morse, R. L. & Neilson, C. W. *Phys. Fluids* **14**, 830–840 (1971).
5. Katsouleas, T. & Dawson, J. M. *Phys. Rev. Lett.* **51**, 392 (1983).
6. Katsouleas, T., Joshi, C., Mori, W. B. & Dawson, J. M. *Proc. 12th int. Conf. on High-Energy Accelerators* (Fermilab, Batavia, 1982).
7. Cohen, E. I., Kaufman, A. N. & Watson, K. M. *Phys. Rev. Lett.* **29**, 581–584 (1972).

Is there a climatic attractor?

C. Nicolis

Institut d'Aéronomie Spatiale de Belgique, 3 avenue Circulaire, 1180 Bruxelles, Belgium

G. Nicolis

Faculté des Sciences de l'Université Libre de Bruxelles, Campus Plaine, Boulevard du Triomphe, 1050 Bruxelles, Belgium

Much of our information on climatic evolution during the past million years comes from the time series describing the isotope record of deep-sea cores. A major task of climatology is to identify, from this apparently limited amount of information, the essential features of climate viewed as a dynamic system. Using the theory of nonlinear dynamic systems we show how certain key properties of climate can be determined solely from time series data.

EXPERIMENTAL data have essentially two roles in the process of modelling. First, they parameterize the equations postulated by the modeller. Second, they set constraints to be satisfied by the model. For instance, a reasonable model of Quaternary glaciations should reproduce the general aspects of a palaeotemperature time series as deduced from ice or deep-sea core data and, in particular, should exhibit the characteristic time scales of 100,000, 41,000 and 22,000 yr (ref. 1). In either case, however, the information drawn from the data will remain esentially one-dimensional. Thus, starting from the time series of a certain variable one may construct a power spectrum or a histogram which, despite their interest, do not provide any hint about the additional variables that may affect the evolution. We show here that experimental data contain far richer information which, independent of any particular model, can be used to 'resurrect' the multivariable dynamics of a system starting from a time series pertaining to a single variable.

We should first comment on the status of a time series from the standpoint of the theory of dynamical systems. Let $X_0(t)$ be the time series available from the data, and $\{X_k(t)\}$, where $k = 0, 1, \ldots n-1$, the full set of variables actually taking part in the dynamics. $\{X_k\}$ is expected to satisfy a set of first-order nonlinear equations, whose form is generally unknown but which, given a set of initial data $\{X_k(0)\}$, will produce the full details of the system's evolution. It is instructive to visualize this evolution in an abstract multi-dimensional space spanned by these variables, the phase space. An instantaneous state of the system becomes a point, say P, in this space, whereas a sequence of such states followed as time varies defines a curve, the phase space trajectory (see Fig. 1). As time grows and transients die out, the system is expected to reach a state of permanent regime, not necessarily time-independent. In phase space, this will be reflected by the convergence of whole families of phase trajectories towards a subset of phase space (C in Fig. 1), such that the system subsequently remains trapped therein. We refer to this invariant set as the attractor.

The interest of the phase space description of a system lies primarily in the fact that the nature of the attractors provides extensive information on the time behaviour of the variables and on the nature of their coupling. For instance, a point

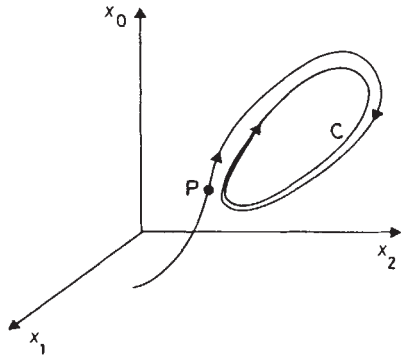

Fig. 1 Typical phase space trajectory emanating from point P and converging to a periodic attractor, represented by curve C.

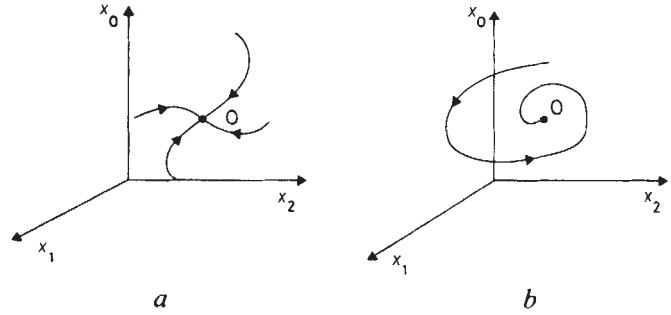

Fig. 2 Two different approaches to a steady state, represented by point 0 in phase space (point attractor). *a*, Monotonic approach; *b*, approach through damped oscillations.

attractor (point 0 in Fig. 2*a*, *b*) implies that the transient-free behaviour of the system will be time-independent. In addition, if the attractor is approached in the way shown in Fig. 2*a* the transients will die out monotonically, whereas a spiral approach like that in Fig. 2*b* indicates that transients perform damped oscillations. An attractor in the form of a closed curve (C in Fig. 1) implies, on the other hand, that the system will perform sustained oscillations in time with an intrinsically-determined period and amplitude. Finally, multiperiodic motions with incommensurate frequencies are represented in phase space by high-dimensional attracting toroidal surfaces. In each of the above cases, the character of the attractor also gives an indication of the minimum number of variables that should be involved in the description. Thus, for the zero-dimensional attractors of Fig. 2 ($d=0$) we need, respectively, at least one variable ($n=1$) for Fig. 2*a* and two variables ($n=2$) for Fig. 2*b*. For the one-dimensional attractor of Fig. 1 ($d=1$) we need at least two variables ($n=2$), and for the simplest quasi-periodic phenomenon we need at least a two-dimensional torus ($d=2$) embedded in a three-dimensional phase space ($n=3$).

So far we have argued in terms of attractors which are points, lines or surfaces or, in more technical terms, smooth topological manifolds characterized by an integer dimensionality. In recent years, it has been firmly established that geometrical objects exist which are not topological manifolds. Such constructions, which have a non-integer dimensionality, are known as fractals[2]. The theory of dynamical systems and some experimental results from fluid dynamics and chemical kinetics provide us with many examples of fractal attractors[3]. The importance of the latter stems from the fact that they model irregular, time-dependent phenomena, characterized by two features, both of which are shared by the climatic system: a marked sensitivity to initial conditions; and the appearance of large dispersions from a mean motion similar to a stochastic process, even though the underlying dynamics is perfectly deterministic. Note that the dimensionality of an attractor, fractal or smooth, is bound to be a number smaller than the number of variables present in the evolution.

Climatic attractor

We shall establish the existence of an attractor associated with the long-term climatic evolution of the past million years and determine its dimensionalty. Knowing the characteristics of this climatic attractor automatically gives us information on the minimum number of variables that must be introduced into the description.

Our starting point is the oxygen isotope record obtained from the equatorial Pacific deep-sea core V28–238 (refs 4, 5), which is one of the best climatic records available, because the sediment accumulated at a fairly regular rate[6].

Let $X_0(t)$ be the corresponding time series[7]. Because the n variables $\{X_k(t)\}$ satisfy a set of first-order differential equations, successive differentiation in time reduces the problem to a single (generally highly nonlinear) differential equation of nth order

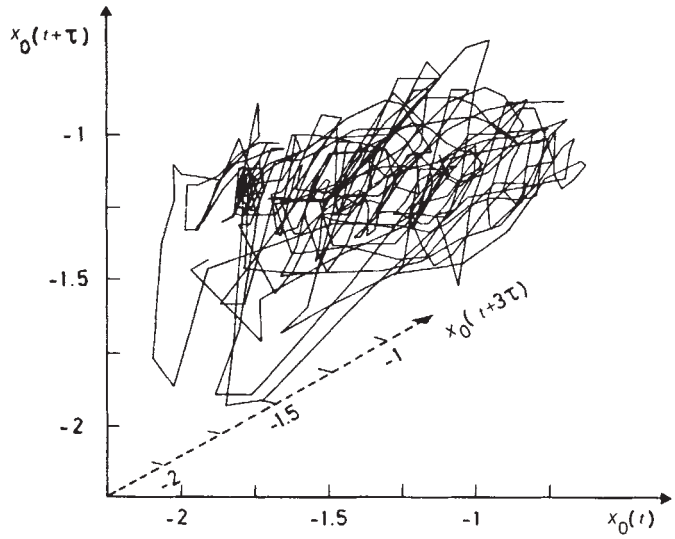

Fig. 3 A view of the climatic attractor embedded in a three-dimensional phase space. The result utilizes about 500 equidistant values of X_0. These are inferred from the oxygen isotope record obtained from the V28-238 deep sea core of Shackleton and Opdyke[4] and extended over the past million years, following an interpolation available from the data bank of the University of Louvain[7]. The value of the shift τ adopted in drawing the figure is $\tau=2$ kyr.

for one of these variables. Thus, instead of $X_k(t), k=0,1,\ldots,n-1$, we may consider $X_0(t)$, the variable supplied by the time series data, and its $n-1$ successive derivatives $X_0^{(k)}(t)$, $k=1,\ldots,n-1$, to be the n variables of the problem spanning the phase space of the system[8]. Now, both X_0 and its derivatives can be deduced from the single time series pertaining to $X_0(t)$, as provided by the data. We see, therefore, that, in principle we have sufficient information at our disposal to go beyond the one-dimensional space of the original time series and to unfold the system's dynamics into a multidimensional phase space.

Actually, as suggested originally by Ruelle[9], instead of $X_0(t)$ and $X_0^{(k)}(t)$ it will be easier to work with $X_0(t)$, and the set of variables obtained from it, by shifting its values by a fixed lag τ. We, therefore, consider from now on the phase space defined by the variables :

$$X_0(t), X_0(t+\tau), \ldots, X_0(t+(n-1)\tau) \qquad (1)$$

For a typical choice of τ these variables are expected to be linearly independent, and this is all one needs to define properly a phase space. A simple example illustrating how an unshifted function can give rise to a linearly independent one by a simple shift is provided by the polynomials $X_0(t)=t^2$, $X_0(t+\tau)=t^2+2t\tau+\tau^2$. These two functions are indeed independent, as

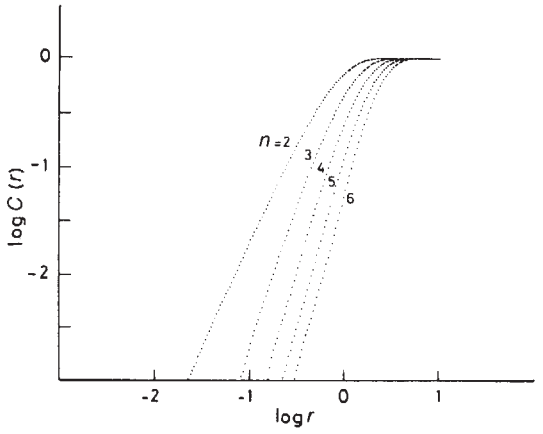

Fig. 4 Distance dependence of the correlation function on the climatic attractor. Note the existence of an extensive range of linearity, from which the dimensionality of the attractor can be inferred. Parameter values as in Fig. 3, except that $\tau = 8$ kyr.

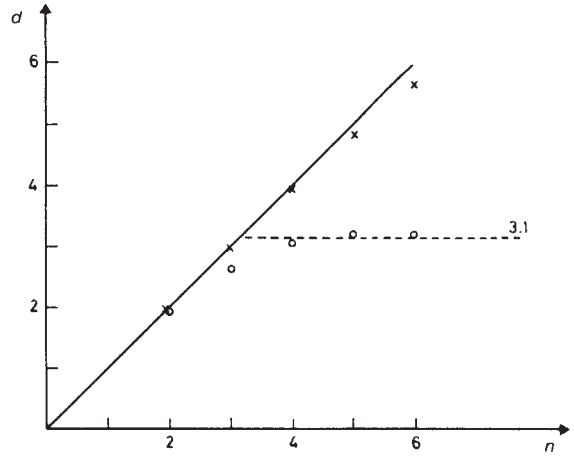

Fig. 5 Dependence of dimensionality, d on the number of phase space variables, n for the climatic attractor (○) and for a white noise signal (×) for the same parameters as in Fig. 4. Notice the saturation to a plateau value of ~3.1 in the first case, and the $d \sim n$ relationship in the second case.

the second polynomial contains terms of first and zero degree in t, which are absent in the first one.

Before describing the procedure that will enable us to obtain quantitative information on the nature of the climatic attractor and, in particular, on its dimensionality we present, in Fig. 3, a characteristic view of this object in a three-dimensional phase space. This view clearly exhibits the complexity of the underlying motion. However, the data are too coarse to draw any conclusion from this figure alone. It will be our task to characterize the complexity of the dynamics more sharply and, in particular, to assess its similarities and differences with random noise. Note that similar phase portraits have been constructed from experimental data pertaining to chemical kinetics[10].

Analytical procedure

We now describe briefly a recently proposed procedure[11,12] which allows the indentification of some salient features of the phase space portrait of a dynamical system. Consider a set of N points on an attractor embedded in a phase space of n dimensions, obtained from a time series:

$$\begin{aligned} &X_0(t_1), \ldots, X_0(t_N) \\ &X_0(t_1+\tau), \ldots, X_0(t_N+\tau) \\ &\quad\vdots \\ &X_0(t_1+(n-1)\tau), \ldots, X_0(t_N+(n-1)\tau) \end{aligned} \tag{2}$$

For convenience we introduce a vector notation: $\mathbf{X}_i$ which stands for a point of phase space whose coordinates are $\{X_0(t_i), \ldots, X_0(t_i+(n-1)\tau)\}$.

A reference point $\mathbf{X}_i$ from these data is now chosen and all its distances $|\mathbf{X}_i - \mathbf{X}_j|$ from the $N-1$ remaining points are computed. This allows us to count the data points that are within a prescribed distance, r from point $\mathbf{X}_i$. Repeating the process for all values of i, one arrives at the quantity

$$C(r) = \frac{1}{N^2} \sum_{\substack{i,j=1 \\ i \neq j}}^{N} \theta(r - |\mathbf{X}_i - \mathbf{X}_j|) \tag{3}$$

where θ is the Heaviside function, $\theta(x) = 0$ if $x < 0$, $\theta(x) = 1$ if $x > 0$. The non-vanishing of this quantity measures the extent to which the presence of a data point $\mathbf{X}_i$ affects the position of the other points. $C(r)$ may thus be referred to as the (integral) correlation function of the attractor.

Suppose that we fix a given small parameter ε and we use it to define the site of a lattice which approximates the attractor. If the latter is a line, the number of data points within a distance r from a prescribed point should be proportional to r/ε. If it is a surface, this number should be proportional to $(r/\varepsilon)^2$ and, more generally, if it is a d-dimensional manifold it should be proportional to $(r/\varepsilon)^d$. We expect, therefore, that for r, relatively small $C(r)$ should vary as

$$C(r) = r^d \tag{4}$$

In other words, the dimensionality d of the attractor is given by the slope of the log $C(r)$ versus log r in a certain range of values of r:

$$\log C(r) = d|\log r| \tag{5}$$

This property remains valid for attractors of fractal dimensionality.

The above results suggest the following algorithm (a similar procedure has also been proposed in the context of fluid dynamics[13,14]):

(1) Starting from a time series, we can construct the correlation function, equation (3), by considering successively higher values of the dimensionality n of phase space.

(2) Deduce the slope d near the origin according to equation (5) and see how the result changes as n is increased.

(3) If d reaches a saturation limit beyond some relatively small n, the system represented by the time series should possess an attractor. The saturation value d_s will be regarded as the dimensionality of the attractor. The value of n beyond which saturation is observed will provide the minimum number of variables necessary to model the behaviour represented by the attractor.

Application to climatic data

This procedure has been applied to the analysis of the data pertaining to core V28–238. Figure 4 gives the dependence of log $C(r)$ versus log r for $n = 2$ to $n = 6$. We see that there is indeed an extended region over which this dependence is linear, in accordance with equation (5). Figure 5 (points in circles) shows that the slope reaches a saturation value at $n = 4$, which is about $d_s = 3.1$. The same plot also shows the way in which d varies with n if the signal considered is a Gaussian white noise: there is no tendency to saturate. In fact, in this case d turns out to be equal to n. It should be emphasized that the above results are independent of the choice of the time lag τ, provided that the latter is of the order of magnitude of the times scales pertaining to the long-term climatic evolution, and the linear independence of the variables is secured.

The existence of a climatic attractor of low dimensionality shows that the main feature of long-term climatic evolution may be viewed as the manifestation of a deterministic dynamics,

involving a limited number of key variables. The fact that the attractor has a fractal dimensionality provides a natural explanation of the intrinsic variability of the climatic system, despite its deterministic character[15]. Moreoever, it suggests that despite the pronounced peaks of spectra in the frequencies of the orbital forcings, the actual behaviour is highly non periodic[16]. A new interpretation of variance spectra of the ice volume record is, therefore, necessary.

Conclusion

We have identified a number of intrinsic properties of the climate assuming it to be dynamical system, using only the time series obtained from the data.

Our results do not anticipate the validity of any particular model of climatic evolution. Rather, they set a number of constraints that should be satisfied by a model. In particular, they suggest that models involving four variables could already provide a description of the salient features of the system.

Our approach could be applied to many other problems in which naturally occurring complex systems are probed through time series. Within the context of atmospheric physics and climatotology, one important example is the blocking transition. Another promising field of application are biological rhythms like the heart beat or the electroencephalogram[17]. In the long run, it may be hoped that fractal dimensionality could become for such systems a useful characterization of their specificity as well as a measure of their complexity.

We thank P. Pestiaux for providing the time series of the V28-238 core and P. Bergé for an enlightening discussion. The work of C.N. is supported, in part, by the EEC under contract no. STI-004-J-C(CD).

Received 2 May; accepted 27 July 1984.

1. Berger, A. L. (ed.) *Climatic Variations and Variability: Facts and Theories* (Reidel, Dordrecht, 1981).
2. Mandelbrot, B. *Fractals: Form, Chance and Dimension* (Freeman, San Francisco, 1977).
3. Helleman, R. (ed.) *Ann. N.Y. Acad. Sci.* **347**, 1981.
4. Shackleton, N. J. & Opdyke, N. D. *Quat. Res.* **3**, 39–55 (1973).
5. Shackleton, N. J. *et al. Nature* **307**, 620–623 (1984).
6. Imbrie, J. *et al.* in *Milankovitch and Climate* (eds Berger, A. L. *et al.*) (Reidel, Dordrecht, 1984).
7. Berger, A. L. & Pestiaux, P. *Tech. Rep.* No. 28, (Institut of Astronomy and Geophysics, Catholic University of Louvain, 1982).
8. Packard, N. H., Crutchfield, J. P., Farmer, J. D. & Shaw, R. S. *Phys. Rev. Lett.* **45**, 712–716 (1980).
9. Ruelle, D. in *Nonlinear Phenomena in Chemical Dynamics*, (eds Pacault, A. & Vidal, C.) (Springer, Berlin, 1981).
10. Roux, J. C., Simoyi, R. H. & Swinney, H. L. *Physica* **8D**, 257–266 (1983).
11. Grassberger, P. & Procaccia, I. *Physica* **9D**, 189–208, 1983.
12. Grassberger, P. & Procaccia, I. *Phys. Rev. Lett.* **50**, 346–349 (1983).
13. Brandstäter, A. *et al. Phys. Rev. Lett.* **51**, 1442–1445 (1983).
14. Malmaison, B., Atten, P., Berge, P. & Dubois, M. *J. phys. Lett.* **44**, 897-902 (1983).
15. Lorenz, E. N. *Tellus* **36A**, 98–110 (1984).
16. Le Treut, H. & Ghil, M. *J. geophys. Res.* **88**, 5167–5190, 1983.
17. Babloyantz, A., Nicolis, G. & Nicolis, J. S. (in preparation).

Structure of the nucleosome core particle at 7 Å resolution

T. J. Richmond, J. T. Finch, B. Rushton, D. Rhodes & A. Klug

MRC Laboratory of Molecular Biology, University Postgraduate Medical School, Hills Road, Cambridge CB2 2QH, UK

The crystal structure of the nucleosome core particle has been solved to 7 Å resolution. The right-handed B-DNA superhelix on the outside contains several sharp bends and makes numerous interactions with the histone octamer within. The central turn of superhelix and H3 · H4 tetramer have dyad symmetry, but the H2A · H2B dimers show departures due to interparticle associations.

THE nucleosome is the primary repeating unit of DNA organization in chromatin[1–3]. Extensive digestion of chromatin with micrococcal nuclease releases the nucleosome core, a small, well-defined particle which has been crystallized. The particle mass (~ 206 kilodaltons) is equally distributed between 146(±2) base pairs (bp) of DNA and an octamer formed by two each of the histone proteins, H2A, H2B, H3 and H4 (the outer histone H1 and the linker DNA having been removed during nuclease digestion[4]). The crystals first obtained were of limited order and gave a picture of the particle to 20 Å resolution[5]. We later prepared better crystals which diffracted to about 5 Å, having a single particle in the asymmetric unit[6]. We describe here the three-dimensional structure of the nucleosome core particle at 7 Å resolution determined by X-ray diffraction and multiple isomorphous replacement. This advance was achieved by improved diffractometry, control of the crystal unit cell parameters by adjustment of hydration, and derivatives prepared from multi-heavy atom cluster compounds.

The nucleosome core crystals have previously been investigated by several structural methods. Electron microscopy and X-ray diffraction techniques were initially used to obtain electron density maps in the principal projections, suggesting that the particle had the shape of a disk 57 Å thick and 110 Å in diameter. The DNA appeared to be wound around the histone core in 1.8 turns of a flat superhelix with a pitch of 28 Å[5]. Using neutron diffraction in conjunction with contrast matching[7,8], the DNA and protein components were seen as separate densities in projections at 25 Å resolution. The three-dimensional shape of the octamer alone was determined to a resolution of 20 Å by image reconstruction from electron micrographs of negatively stained, ordered aggregates[9]. The assignment of histone locations on the resulting low-resolution map relied on DNA–histone[10,11] and histone–histone (for references, see ref. 12) proximities obtained from chemical cross-linking experiments, and the neutron experiments fixed the orientation of the DNA superhelix on the octamer. The suggested division of the octamer into two H2A · H2B dimers residing on opposite faces of a H3 · H4 tetramer agrees well with the pattern of dissociation found in earlier physicochemical studies[13,14]. The tetramer (proteolysed) and octamer have also been crystallized in the absence of DNA, but structures have not yet been reported[15,16].

The electron density map at the higher resolution of 7 Å described here reveals many new structural features. The DNA is not bent uniformly into the superhelix, but exhibits several regions of tight bending or possible kinking, adjacent to points of substantial contact with histones H3 and H4. The histone–DNA interactions occur on the inside of the superhelix; the protein density does not seem to embrace the outside of the